Article

Sol-gel based titania-silica thin film overlay for long period fiber grating-based biosensors

Francesco Chiavaioli, Palas Biswas, Cosimo Trono, Sunirmal Jana, Somnath Bandyopadhyay, Nandini Basumallick, Ambra Giannetti, Sara Tombelli, Susanta Bera, Aparajita Mallick, and Francesco Baldini

Anal. Chem., **Just Accepted Manuscript** • DOI: 10.1021/acs.analchem.5b01841 • Publication Date (Web): 08 Nov 2015

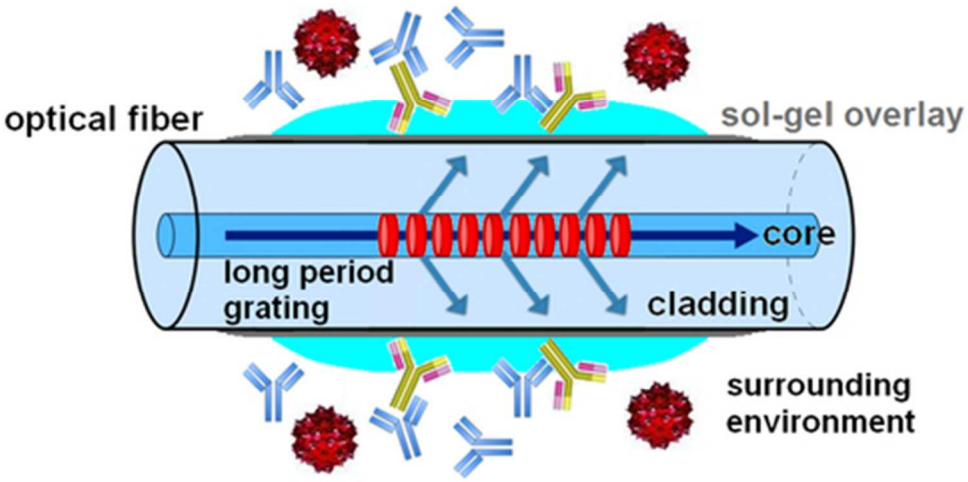

Abstract graphic
40x20mm (300 x 300 DPI)

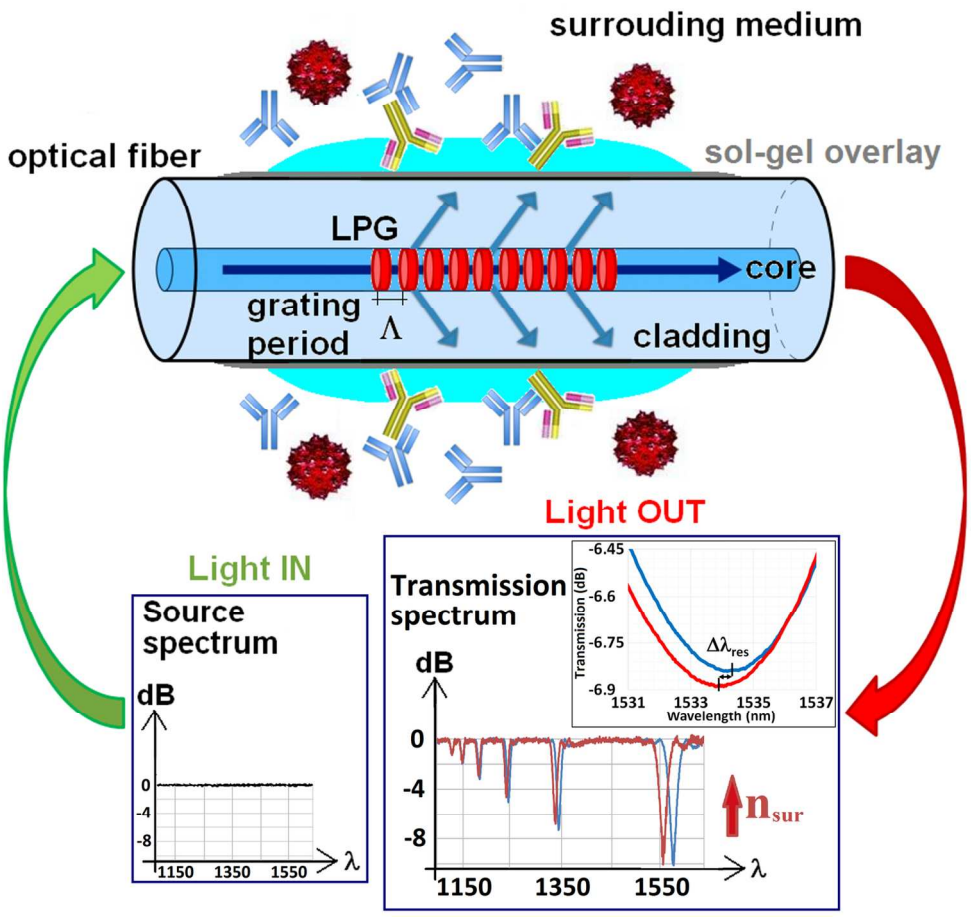

Schematic illustration of the light coupling inside an optical fiber LPG and of the effect of surrounding RI changes on the transmission spectrum. The inset shows the wavelength shift due to a binding interaction.
135x123mm (300 x 300 DPI)

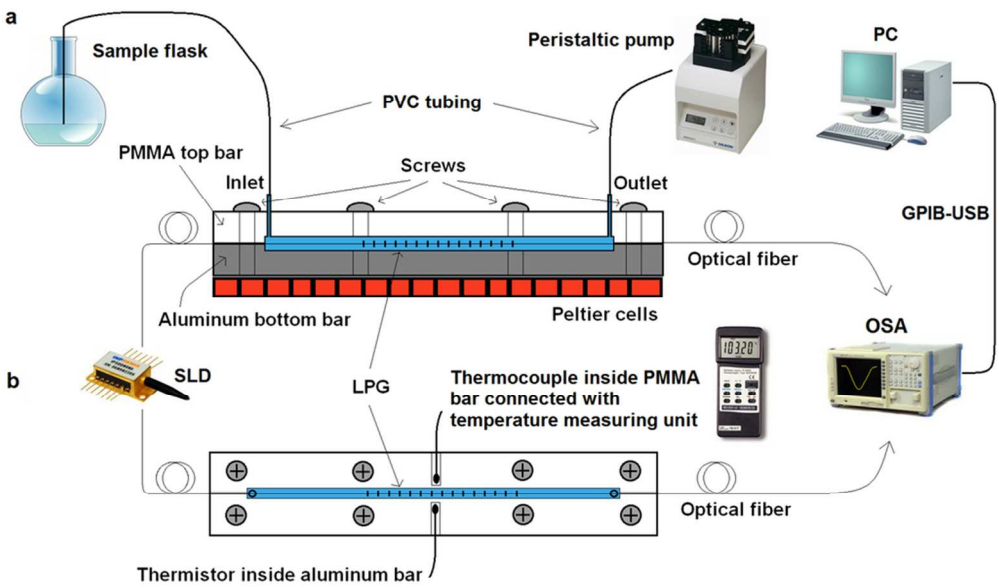

Sketch of the experimental setup together with the cross-section (a) and top view (b) of the thermo-stabilized flow cell.
86x51mm (300 x 300 DPI)

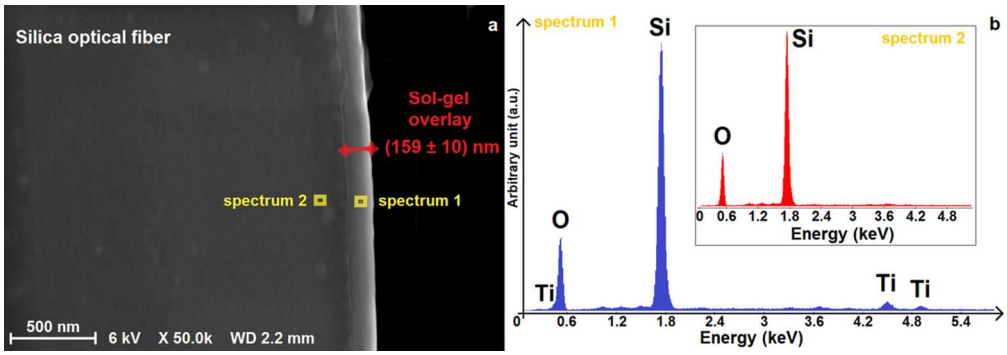

FESEM image of the cross-section (a) of an optical fiber coated with sol-gel based titania-silica film overlay. The image refers to a sensor of batch C (withdrawal speed of 2.9 mm s-1 and sol viscosity of 24.5 mPa·s) from which two portions highlighted in yellow (spectrum 1 in the overlay region and spectrum 2 in the fiber region) are used for X-EDS microanalysis. Blue-colored X-EDS spectrum of all elements present in specimen (b) in the film overlay region. The inset of (b) shows the red-colored X-EDS spectrum of the same sensor considering the fiber (cladding) region.
102x35mm (300 x 300 DPI)

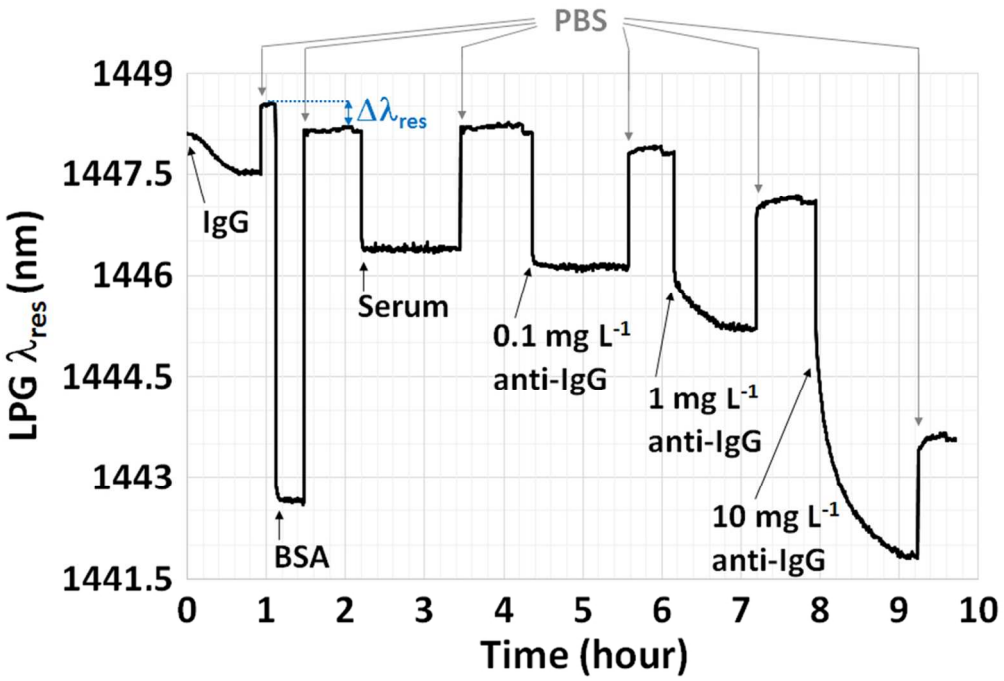

Response of a sol-gel based titania-silica coated LPG of batch C in human serum when the sample was spiked with the antigen (anti-IgG) at 0.1 mg L-1, 1 mg L-1 and 10 mg L-1. The wavelength shift Δλres, highlighted in blue, is related to the blocking of surface free functionalities with BSA agent. All the solution exchanges are indicated with arrows (downward grey arrows for PBS buffer solution, whereas black arrows for all the other reagents).
100x67mm (300 x 300 DPI)

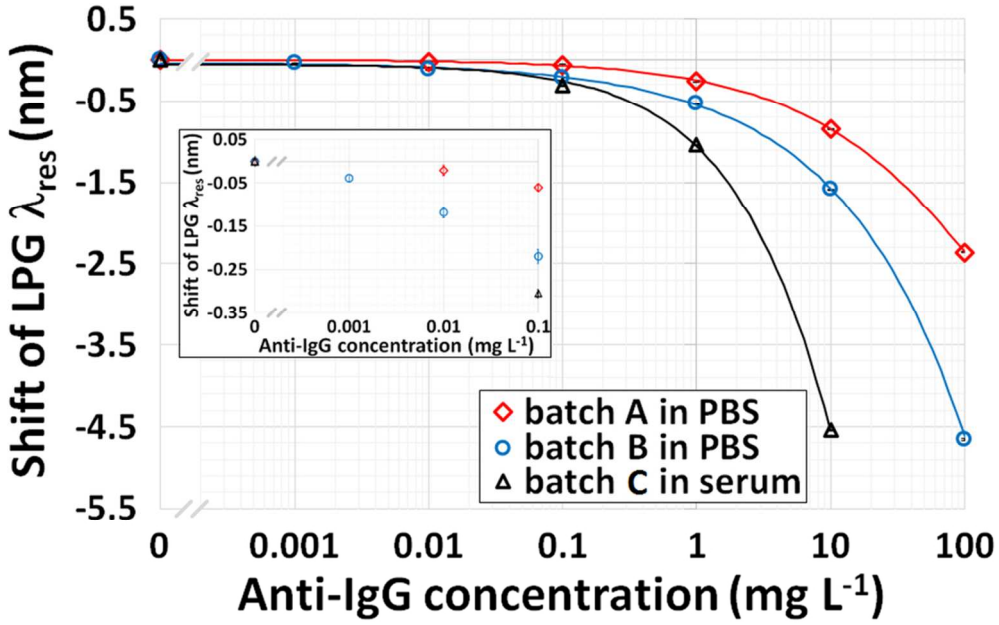

Calibration curves of the proposed biosensor either in buffer or in serum obtained by using the same assay protocol with different sol-gel based titania-silica coated LPGs: LPGs of batches A (red rhombuses) and B (blue circles) by performing the assay in PBS buffer, and of batch C (black triangles) by performing the assay in human serum. The solid lines provide the best logistic fit of the experimental data. The inset shows the shift of the LPG λ_{res} at the lower concentrations of analyte.
92x57mm (300 x 300 DPI)

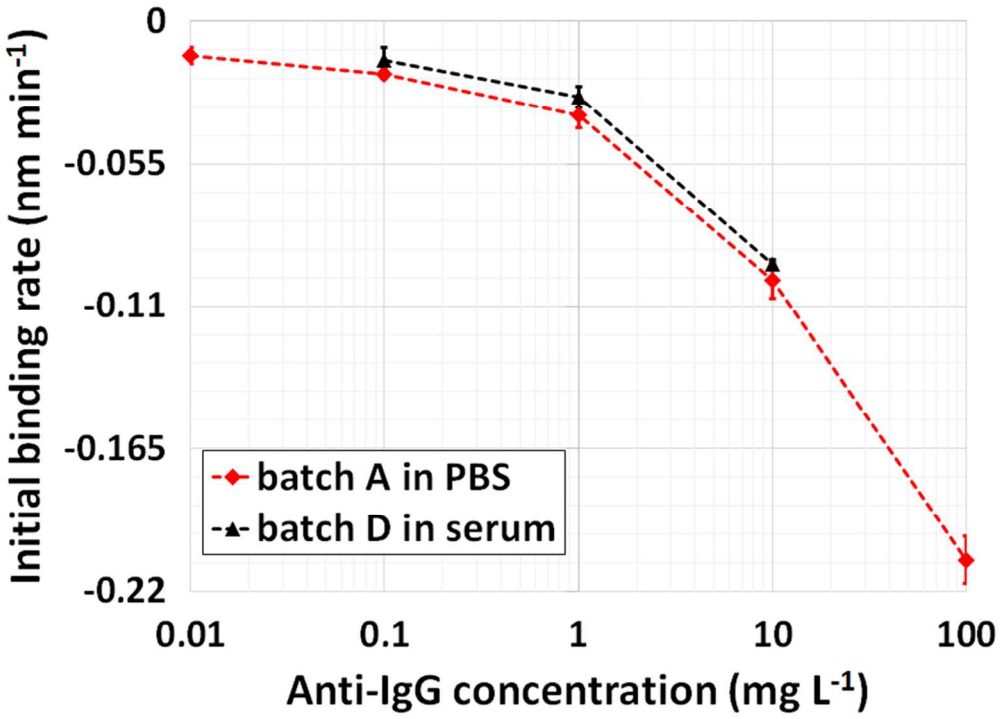

Calibration curves of the proposed biosensor (IBR vs antigen concentration in logarithmic scale) obtained by using the same procedure but with different coated LPGs: LPG of batch A (red rhombuses) by performing the assay in PBS buffer, and of batch C (black triangles) by performing the assay in human serum. The dashed lines are the broken lines that connect the experimental points and are drawn with the purpose to provide a general view of the trends.
106x76mm (300 x 300 DPI)

Sol-gel based titania-silica thin film overlay for long period fiber grating-based biosensors

Francesco Chiavaioli,[†] Palas Biswas,[,‡] Cosimo Trono,[*,†] Sunirmal Jana,[‡] Somnath Bandyopadhyay,[‡] Nandini Basumallick,[‡] Ambra Giannetti,[†] Sara Tombelli,[†] Susanta Bera,[‡] Aparajita Mallick,[‡] and Francesco Baldini[†]*

[†]Institute of Applied Physics "Nello Carrara", CNR-IFAC, Via Madonna del Piano 10, 50019 Sesto Fiorentino (FI), Italy

[‡]Central Glass and Ceramic Research Institute, CSIR-CGCRI, 196 Raja S C Mullick Road, Kolkata 700032, India

ABSTRACT: An evanescent wave optical fiber biosensor based on titania-silica coated long period grating (LPG) is presented. The chemical overlay, which increases the refractive index (RI) sensitivity of the sensor, consists of a sol-gel based titania-silica thin film, deposited along the sensing portion of the fiber by means of the dip-coating technique. By changing both the sol viscosity and the withdrawal speed during the dip-coating, it was possible to adjust the thickness of the film overlay, which is a crucial parameter for the sensor performance. After the functionalization of the fiber surface using a methacrylic acid/methacrylate copolymer, an antibody/antigen (IgG/anti-IgG) assay was carried out to assess the performance of sol-gel based

titania-silica coated LPGs as biosensors. The analyte concentration was determined from the wavelength shift at the end of the binding process and from the initial binding rate. This is the first time that a sol-gel based titania-silica coated LPG is proposed as an effective and feasible label-free biosensor. The specificity of the sensor was validated by performing the same model assay after spiking anti-IgG into human serum. With this structured LPG, detection limits of the order of tens of $\mu g\ L^{-1}$ (10^{-11} M) are attained.

KEYWORDS: Optical fiber biosensor, Long period grating, Sol-gel, Titania-silica thin film overlay, Label-free immunoassay, Serum.

INTRODUCTION

The development of real-time methods, particularly label-free biosensors, which combine high sensitivity and selectivity for the recognition of low concentrations of analytes with rapid response and long-term stability is a groundbreaking field both in fundamental and in applied research, such as in healthcare diagnostics.[1–2]

When a label-free detection of chemical compounds or biological species is carried out using an optical transduction approach, the working principle is the modulation of the optical signal induced by the change of the refractive index (RI) occurring at the liquid/solid sensor interface, where the sensing layer interacts with the analyte under investigation. Generally, the modification of the optical signal arises from the interaction of the evanescent wave with the sensing layer. The literature accounts for several optical configurations, mainly based on surface plasmon resonance (SPR),[3–5] on localized SPR,[6–7] on interferometry[8] or on optical resonance.[9]

The substrate on which the sensing layer is deposited is generally either a planar chip[10] or an optical fiber.[11–12]

Recently, optical fiber long period gratings (LPGs) have been proposed as a promising tool for label-free biosensors.[13–22] Compared to the other kinds of resonance-based optical sensors (e.g. microspheres, microbubbles, etc.), LPGs are easier to be manufactured, more robust, and exploit the peculiarities of optical fibers, such as compactness, lightweight, intrinsic miniaturization, high compatibility with optoelectronic devices, remote measurement capabilities and multiplexing thanks to the spectral modulation of the signal.

Due to periodic RI perturbations induced in the core of a single-mode optical fiber, LPGs enable the coupling of the fundamental core mode to co-propagating cladding modes at well-defined resonance wavelengths (LPG λ_{res}). Therefore, the transmission spectrum of an LPG will be characterized by one or more attenuation bands (Figure 1), in which the minimum of each band corresponds to the coupling with a selective *m*-th cladding mode when the phase-matching condition is satisfied, as expressed by the characteristic equation of LPGs[23]

$$\lambda_{res(m)} = (n_{eff,core} - n_{eff,clad(m)}) \Lambda \quad (1)$$

Here, Λ is the grating period (usually in the range from 100 μm to 600 μm), $n_{eff,core}$ and $n_{eff,clad(m)}$ represent the effective RIs of the fundamental core mode (i.e. LP_{01}) and the *m*-th cladding mode (i.e. LP_{0m}), respectively. $n_{eff,clad}$ depends on the RI of the surrounding medium (n_{sur}) and this relationship allows to exploit LPGs as RI sensors.

As sketched in Figure 1, the optical mechanism of LPG-based biosensing can be explained considering that the binding interactions produce a shift of the attenuation band, and consequently a shift of the LPG λ_{res} (i.e. $\Delta\lambda_{res}$, from the blue curve to the red one as shown in the

inset of Figure 1) due to an increase of the $n_{eff,clad}$ (see eq. 1), which is in turn related to the increase of both n_{sur} and the thickness of the bio-overlay itself.

Figure 1. Schematic illustration of the light coupling inside an optical fiber LPG and of the effect of surrounding RI changes on the transmission spectrum. The inset shows the wavelength shift due to a binding interaction.

The best RI sensitivity of LPGs is reached when n_{sur} is close to the RI of fiber cladding (i.e. 1.44–1.46 RIU, RI unit), thus quite far from the RI of water or aqueous solutions (i.e. 1.33–1.34 RIU).[24] To overcome this problem, the literature accounts for a general approach that consists in the deposition over the fiber of a nm-thick film overlay of RI higher than the cladding RI.[25–27] By properly tuning both the RI and the thickness of the deposited overlay, the RI range in correspondence of the maximum sensitivity can be adjusted around 1.33 RIU.[28–29] In this case, values of RI sensitivity of the order of thousands of nm RIU^{-1} can be experimentally achieved.[30]

Sol-gel-derived coatings have been used for years to enhance the performance of evanescent wave sensors since they are characterized by an intrinsic porosity, which increases the available surface for the immobilization of the bioreceptor and, consequently, the sensitivity of the sensors.[31–34] Sensor manufacturing is quite simple thanks to the dip-coating (DC) technique,[31,35] which offers great flexibility in the process parameters and precursors, making it possible to produce tailored values of the material properties and thickness that can have a strong impact in the sensor performances. Moreover, the possibility of doping sol-gel coatings with high refractive index materials provides the chance for implementing high RI (HRI) film overlay with good and stable optical characteristics, suitable to be applied to LPG sensors. An interesting

example of HRI overlay reports the use of diamond-like carbon nano-coatings for improving the sensing performance of LPGs,[36] while another one shows the RI sensing capability of LPGs coated with an Al_2O_3 overlay.[37] A HRI overlay of TiO_2 was recently detailed in order to optimize the sensing characteristics of LPGs for the detection of bacteria endotoxin.[38] Considering LPG-based devices, up to now sol-gel based titania-silica film overlays have been used for gas sensing[39] and for the development of optical refractometers.[35]

In the present paper, the performances of an LPG-based biosensor utilizing a sol-gel based titania-silica thin film as coating were investigated. The HRI film overlay, deposited by means of the DC technique along the sensing portion containing the LPG improved the sensor performance in terms of volume RI sensitivity (optical refractometer), and of bio-layer formation sensitivity (biosensor). An IgG/anti-IgG assay implemented by immobilizing IgG on the HRI thin film overlay was used as a model assay to characterize the LPG biosensor with calibration curves obtained both in buffer and in serum.

EXPERIMENTAL SECTION

Manufacturing of Long Period Gratings

LPGs with Λ of 342 μm were manufactured in a standard single-mode fiber (SMF28e of Corning Inc.) using point-to-point inscription technique[40] by means of a KrF pulsed Excimer laser (Braggstar-500, TUI laser, Germany) operating at a wavelength of 248 nm, with a repetition rate of 200 Hz and an energy per pulse of 8–10 mJ. Before inscription, the fiber was hydrogen loaded at a pressure of 1500 psi (10.34 MPa) and a temperature of 100 °C for 48 hours to enhance the photosensitivity. For applications at room temperature, after the UV inscription, an annealing process at 150–170 °C for about six hours is required to stabilize the optical

characteristics of LPGs.[41] An example of how the annealing process affects the LPG spectrum (solid blue line) is shown in Figure S-1 in which the stabilization and consolidation of the attenuation bands can be observed after the heat treatment (solid red line). In order to deposit a glassy coating (e.g. a sol-gel based thin film overlay) over an optical fiber containing an LPG, the grating region must be heated at around 450 °C during sintering the gel film. In general, at that temperature, an LPG becomes unusable because the attenuation bands almost reduce to zero. To overcome this, during the grating manufacturing, we intentionally over-coupled the cladding mode of interest (i.e. LP_{07}) with a greater coupling strength (details in Supporting Information) thus to achieve stable LPGs when heated.[42] The LPGs were stabilized at 550 °C and then gratings with an LPG λ_{res} of 1580–1610 nm, with a visibility of the attenuation band from -10 dB to -14 dB, and with a full width at half maximum (FWHM) bandwidth of 18–22 nm were attained at the resonance condition (see eq. 1) for the LP_{07} cladding mode.

Preparation of Precursor Sol and Deposition of Titania-Silica Thin Film on LPGs

The process of sol-gel preparation is well-known and was recently illustrated in detail.[43] For the silica sol (10 wt% silica) preparation, TEOS was mixed with 1-propanol with distilled water in presence of 1 N HCl as catalyst (molar ratio, water:TEOS:HCl = 2:1:0.001). For the titania sol, TIOT was drop-wise added with 2-propanol and acetyl acetone as sol stabilizing agent (molar ratio, acetyl acetone:TIOT = 1:2). The two sols were mixed by stirring for about 4 hours and then kept to age for additional 24 hours. The Ti:Si ratio and the total equivalent oxide weight percentage (wt.%) were 1:1 and 7.3, respectively. The viscosity of the 24 hours-aged sol was measured by using a rheometer (Thermo scientific, Germany, Haake RheoStress 6000) at 27 °C. To obtain thicker film, the viscosity of the sol (24 hours-aged sol) was widely increased from

(3.2 ± 0.1) mPa·s up to (27.0 ± 0.5) mPa·s by controlling the evaporation of the solvents through the warming of the sol at (65 ± 5) °C.

Considering the Ti:Si volumetric ratio (1:1), a layer RI of ~1.7 RIU can be estimated as the mean value between the titania RI (i.e. 1.91–1.96 RIU) and silica RI (i.e. 1.42–1.44 RIU).[35] To optimize the sensor performance and to reach the optimum overlay thickness (OOT), the film thickness was varied by changing both the sol viscosity during the sol preparation and the withdrawal speed during the film deposition. A single layer (thus a single deposition step) was found to be adequate to move the selected cladding mode to its transition region.[25,44]

Afterwards, the LPG was heated in a furnace (MTI furnace, USA) in order to allow the oxide formation in the deposited film. During the heat treatment, the temperature of the furnace was increased from 26 °C to 450 °C at a rate of about 1.2 °C min^{-1} and then the LPG was kept at 450 °C for about 2.5 hours. Later, the furnace temperature was slowly cooled down with the same rate of 1.2 °C min^{-1} in order to avoid any crack due to thermal shock. At the end of the process, the LPG wavelength of LP_{07} mode was measured in air and in phosphate buffered saline (PBS) solution.

To confirm the deposition of the sol-gel film overlay over the sensing portion of the fiber, a field emission scanning electron microscope (FESEM) was used (FESEM; Supra 35VP, Carl Zeiss) along with the X-ray energy dispersive spectroscopy (X-EDS) FESEM tool.

Experimental Setup

The experimental setup is shown in Figure 2 together with the thermo-stabilized flow cell[45] in its cross-section (Figure 2a) and top view (Figure 2b). The flow cell (50 μL total volume) consists of two parts: the PMMA top bar and the aluminum bottom, with this one in thermal contact with a thermo electric cooler (TEC). The optical fiber containing the LPG is glued at

both the edges of the flow cell and a thermocouple (Lutron TM-917) records the temperature of the measurement environment. Each sample contained into the flask is pumped inside the flow cell by means of a peristaltic pump (Gilson Minipuls 3). The light is launched by a broadband superluminescent diode (SLD) INPHENIX IPSDD1401 or IPSDD1503 (1410 nm or 1550 nm central wavelength, respectively, and 60 nm FWHM bandwidth) depending on the value of LPG λ_{res}. The light is acquired by an optical spectrum analyzer (OSA) Anritsu MS9030A – MS9701B (0.1 nm spectral resolution). Finally, an in-house made software program allows recording both the temperature and the spectrum from which the value of the LPG λ_{res} is determined using the Lorentzian fitting function with an acquisition time of 20 s and with a resolution of few picometers arising from the fitting process.[45] Figure S-2 details an example of the above-mentioned fitting procedure. A comprehensive description about the overall data processing and analysis is provided in Supporting Information.

Figure 2. Sketch of the experimental setup together with the cross-section (a) and top view (b) of the thermo-stabilized flow cell.

In correspondence of the LPG coated with the sol-gel film, a layer of Eudragit L100 copolymer was deposited in order to provide functional groups (-COOH) for antibody immobilization.[18] Once the sol-gel based titania-silica coated LPG was functionalized, the optical fiber was placed inside the flow cell. All the steps for the implementation of the immunoassay, detailed in Supporting Information and schematized in Figure S-3, were performed at 23 °C.

Sensor Response to Temperature and Refractive Index Variations

In order to provide an overview of the general characteristics of the proposed biosensor and prior to analyze the device as immunosensor, the response of LPGs from different batches to temperature and volume RI changes was determined. For the temperature characterization, the temperature of the flow cell was varied between 20 °C and 26 °C with steps of 1 °C. The sensor was kept in air in the first experiment, then was surrounded by deionized water at a RI of 1.333 RIU (1.315 RIU at 1550 nm).[46] Due to the thermo-optic effect acting on water (-8 x 10^{-5} RIU ºC^{-1}),[47] the RI was not constant but decreased of 4.8 x 10^{-4} RIU at the end of the second temperature characterization. This effect was taken into account and the temperature analysis was conducted accordingly. For the RI characterization, the surrounding RI was varied at a fixed temperature of 23 °C by means of NaCl-in-water solutions of known RI: from 0.1% wt., 1.333 RIU up to 0.6% wt., 1.334 RIU (1.316 RIU at 1550 nm),[46] with step of 0.1% wt. Each measurement was taken at flow stopped when the temperature was stable with fluctuations lower than 0.03 ºC. After each measurement, the fiber was rinsed with deionized water at high flow rate (500 μL min^{-1}) for 10 minutes in order to remove any remaining NaCl on the overlay surface. It is worth noting that the values of RIs specified in this work have to be considered at the sodium line wavelength (589 nm), unless otherwise stated.

RESULTS AND DISCUSSION

Sol-gel based titania-silica thin film overlay: imaging and analysis

Different coatings were realized by changing the withdrawal speed during the DC and the sol viscosity.[35] If a slow withdrawal speed is used, the sol has more time to drain from the substrate and, consequently, a thinner film overlay is deposited; on the contrary, if a high withdrawal speed is used, the sol has less time to drain and more particles are deposited on the surface

leading to a thicker film overlay. Moreover, the oxide concentration of the sol, which affects the sol viscosity, also has an effect on the overlay thickness.[48]

Table 1 shows different types of coatings, having the same composition of sol (titania:silica = 1:1), grouped in three different batches (A, B, C) on the basis of the sol viscosity, of the used withdrawal speed and of the shift of LPG λ_{res} measured in air after the film coating for all the batches.

Table 1. Characteristics of sol and film deposition parameter for the film overlay deposited on LPGs, along with the wavelength shift of the LP_{07} mode measured in air after the film coating.

Batch	Sol viscosity	Withdrawal speed	LPG λ_{res} shift after sol-gel coating
	mPa·s	mm sec^{-1}	nm
A	3.2	2.5	8
B	27.0	2.2	13.5
C	24.5	2.9	20

An overlay RI of about 1.7 RIU was estimated, which agrees with the values detailed in other works.[35,16] To confirm this, the RI value of the final coating material was calculated considering the shift of the LPG λ_{res} before and after the sol-gel deposition.[25,29] Focusing on the cladding mode of interest, i.e. LP_{07}, and considering a sensor of batch C, a shift of the LPG λ_{res} of 20 nm (Figure S-4) was achieved, which means an overlay RI of 1.698 RIU, estimated through calculations[49] considering the shift of the LPG λ_{res} and an average overlay thickness of 160 nm as later detailed.

FESEM was used to analyze the characteristics of the film overlay. Figure 3a shows an image of the cross-section of an optical fiber coated with the sol-gel based titania-silica film overlay (sensor of batch C). Using FESEM software tools, the thickness of the deposited sol-gel film

overlay was estimated as (159 ± 10) nm, highlighted in red in Figure 3a by the + symbols and the straight line. The surface homogeneity was also evaluated: very little sol-gel conglomerates with dimensions lower than 200 nm are present. Similar results were obtained for all the other batches listed in Table 1 (data not shown). The surface homogeneity is further demonstrated by the conserved characteristics of the LPG spectrum after the film deposition: no losses or very small ones (<0.5 dB) are visible in both the global attenuation value and the visibility of the attenuation band. This is true for all the sensors belonging to each batch (see Figure S-4 in Supporting Information).

Figure 3. FESEM image of the cross-section (a) of an optical fiber coated with sol-gel based titania-silica film overlay. The image refers to a sensor of batch C (withdrawal speed of 2.9 mm s^{-1} and sol viscosity of 24.5 mPa·s) from which two portions highlighted in yellow (spectrum 1 in the overlay region and spectrum 2 in the fiber region) are used for X-EDS microanalysis. Blue-colored X-EDS spectrum of all elements present in specimen (b) in the film overlay region. The inset of (b) shows the red-colored X-EDS spectrum of the same sensor considering the fiber (cladding) region.

In order to complete the analysis of the film overlay, two portions of the same sensor of batch C, highlighted in yellow in Figure 3a (spectrum 1 in the overlay region and spectrum 2 in the fiber region) were used for the X-EDS microanalysis. Figure 3b shows the blue-colored X-EDS spectrum of all elements present in specimen in the film overlay region, whereas the inset details the red-colored X-EDS spectrum of the same sensor considering the fiber (cladding) region. Through the X-EDS, it was possible to confirm the presence of titanium in the overlay region (spectrum 1) with a total amount of 6% as detailed by the energy peaks at 0.44 keV, 4.51 keV

and 4.92 keV, respectively. Conversely, no presence of titanium is shown in the fiber region (spectrum 2). Considering the chemical elements constituting the sol, the percentage of titanium evaluated by X-EDS and by assuming similar penetration coefficients of X-rays into the three elements (i.e. oxygen, silicon and titanium) present in the cured film, an overlay thickness of (154 ± 10) nm could be estimated in agreement with the thickness measured by FESEM imaging in Figure 3a.

The thickness and RI of the overlay depend on many factors such as the sol composition, sol ageing time, withdrawal speed during DC as well as the film curing temperature.[48,50,51] By looking at Figure S-5 and S-6, the sensor will show similar performance in terms of sensitivity if it operates along the linear region of the transition curve of LP_{07} mode (effective RI vs. overlay thickness). Comparable characteristics of the sensor performance were obtained within ±15 nm of thickness and ±1% of RI by repeating several times the film deposition.[52]

Sensor thermal cross-sensitivity, volume refractive index sensitivity and long-term stability

The temperature-related study (details in Supporting Information) demonstrated that the thickness of the film overlay does not influence the temperature sensitivity, a known characteristic of LPGs, and that the temperature sensitivity of sol-gel based titania-silica coated LPGs, which is (0.13 ± 0.01) nm $°C^{-1}$ in air, is slightly higher than standard not coated LPGs (0.1 nm $°C^{-1}$).[53] If the same experiment is conducted in water, the temperature sensitivity increases up to (0.27 ± 0.01) nm $°C^{-1}$ due to the thermo-optic effect. In fact, even if the response of these sensors to temperature variations in air is useful to understand the LPG response by itself, the measurement performed in water environment is essential since mimics the real experimental conditions during the immunoassay. In any case, the contribution related to the thermo-optic effect was taken into account and removed from each experiment.

Although the performances of the proposed biosensor depend on the RI changes that occur on the sensor surface during the antibody/antigen interactions, a volume (or bulk) RI characterization is significant for an exhaustive comprehension of the sensor performances.[13] A comparison considering the same LP_{07} cladding mode was carried out for three different LPGs (not coated, batch A and B) in the RI range between 1.333 RIU ad 1.334 RIU using NaCl solutions. Table 2 provides the shift of LPG λ_{res}, the RI sensitivity, the maximum experimental standard deviation σ of measurements and the resolution attained considering three times the standard deviation divided by the sensitivity.[45]

Table 2. Comparison of the results achieved using different sol-gel based titania-silica coated LPGs in terms of bulk RI characterization.

Batch	LPG λ_{res} shift	Bulk sensitivity	σ	Resolution
	nm	nm RIU^{-1}	pm	RIU
not coated LPG	-0.03	-29.8	8	8.1×10^{-4}
A	-2.02	-2044.5	10	1.5×10^{-5}
B	-7.03	-7075.3	11	4.6×10^{-6}

As shown in Table 2, there is a great enhancement (both sensitivity and resolution), going from a simple not coated LPG to a coated LPG. Moreover, by optimizing the thickness of the film overlay with values around 130–175 nm and thus towards the OOT considering PBS as surrounding medium (RI of 1.334 RIU or 1.317 RIU at 1550 nm), it is possible to achieve good performances. The method adopted to optimize the sensitivity of sol-gel based titania-silica coated LPGs as a function of the overlay thickness is described in detail in Supporting Information (Figure S-5, S-6 and S-7). The resolution detailed in Table 2 takes into account both

the error due to the fit and the system stability since it is calculated considering the standard deviation of 15 subsequent acquisitions for each sample in the same experimental conditions (further details in Supporting Information). Moreover, the precision on the estimation of the LPG λ_{res} was evaluated by measuring the signal from the sensor of batch B used in the RI calibration (Table 2) on 10 independently-prepared solutions of PBS. A mean value of 1533.667 nm and a standard deviation of 15 pm were obtained, leading to a precision of 15 pm (relative error of 0.001%).

The long-term stability, depending both on the intrinsic characteristics of the sensor and on the quality of thermal stabilization of the microfluidic system, was investigated in water environment. The sensor drift, setting the temperature of the flow cell at 23 °C, was 0.3 pm h^{-1} (0.2 pm h^{-1} after removing the contribution of the thermo-optic effect) with the experimental standard deviation on a time window of five hours equal to 10 pm (Figure S-8), which is comparable with the standard deviations obtained in the immunoassay experiments (see Immunoassay Section). Comparable values of the sensor drift were attained for the LPGs coming from all the other batches (within 1%; data not shown). As shown in Figure S-8 (solid grey line), the maximum fluctuation of temperature was 0.07 °C.

The effect of temperature fluctuations on a long-term RI sensing was also studied. The thermo-optic effect acting on solutions should be taken into account for each sensor having high RI sensitivity (greater than thousands of nm RIU^{-1}). In fact, to obtain resolution down to 4×10^{-6} RIU, the temperature variations during the experiment should be lower than 0.05 °C. With the developed experimental setup, temperature fluctuations of 0.03 °C were recorded during all the measuring steps that in turn mean temperature-induced RI changes lower than the best resolution (Table 2).

Immunoassay

The immunoassay was carried out with three sol-gel based titania-silica coated LPGs, each coming from the three batches (A, B and C), either in PBS (LPGs of batches A and B) or in serum (LPG of batch C). By monitoring the dynamic interactions occurring during all the steps of the assay, real-time sensorgrams (LPG λ_{res} evolution in time) can be obtained.

Figure 4 shows the response of a coated LPG of batch C in human serum when the sample was spiked with the antigen (anti-IgG) at 0.1 mg L^{-1}, 1 mg L^{-1} and 10 mg L^{-1}. The blocking of all the surface free functionalities with BSA generated a decrease of LPG λ_{res} of $\Delta\lambda_{res}$ = 0.36 nm ± 0.01 nm highlighted in blue in Figure 4. On the other hand, the injection of serum generated a negligible decrease of LPG λ_{res} of 0.015 nm ± 0.01 nm (in PBS before and after serum) not evident in Figure 4, demonstrating a low non-specific interaction of the components of the serum matrix. Each washing step with PBS, indicated with downward grey arrows in Figure 4, is necessary for measuring the real wavelength shift related only to the interactions between the sensing bio-layer and the sample (surface RI changes). The duration of the whole immunoassay, including the antibody immobilization step, was of several hours, but the long-term stability of the sensing system, previously discussed, guarantees the absence of any disturbance.

Figure 4. Response of a sol-gel based titania-silica coated LPG of batch C in human serum when the sample was spiked with the antigen (anti-IgG) at 0.1 mg L^{-1}, 1 mg L^{-1} and 10 mg L^{-1}. The wavelength shift $\Delta\lambda_{res}$, highlighted in blue, is related to the blocking of surface free functionalities with BSA agent. All the solution exchanges are indicated with arrows (downward grey arrows for PBS buffer solution, whereas black arrows for all the other reagents).

Figure 5 shows the three calibration curves (LPG λ_{res} shift as a function of log concentration of antigen) for anti-IgG obtained by means of the best logistic fit[54] (solid lines) of the experimental points with the immunoassay implemented either in PBS (LPG of batch A, red rhombuses, and LPG of batch B, blue circles) or in human serum (LPG of batch C, black triangles). The figure inset details the shift of the LPG λ_{res} at the lower concentrations of analyte for all the calibration curves.

Figure 5. Calibration curves of the proposed biosensor either in buffer or in serum obtained by using the same assay protocol with different sol-gel based titania-silica coated LPGs: LPGs of batches A (red rhombuses) and B (blue circles) by performing the assay in PBS buffer, and of batch C (black triangles) by performing the assay in human serum. The solid lines provide the best logistic fit of the experimental data. The inset shows the shift of the LPG λ_{res} at the lower concentrations of analyte.

Each experimental point, which was taken with flow stopped at the end of each PBS washing, is the average of fifteen subsequent measurements, whereas each fitting curve provides a correlation greater than 0.99. For all the fitting curves, the value of maximum experimental standard deviation (0.015 nm) is comparable with the maximum deviation of residuals (0.018 nm), testifying the quality of the entire measuring procedure. Limits of detection (LOD), calculated as three times the standard deviation of the blank measurement, of 25 μg L^{-1} (LPG of batch A) with a total wavelength shift (TWS) of 2.36 nm, of 13 μg L^{-1} (LPG of batch B) with a TWS of 4.66 nm and of 8 μg L^{-1} (LPG of batch C) with a TWS of 4.55 nm (final concentration of 10 mg L^{-1}) were attained. The LOD of 8 μg L^{-1} is nine-fold lower than that achieved in the same experimental conditions (i.e. human serum) but using a not coated LPG, as previously

reported.[22] In addition, the results obtained using a coated LPG of batch B compared to that one of batch A prove that the optimization of the overlay thickness is crucial in the case of optical platforms based on coated LPGs, not only for the bulk RI sensitivity but also in their use as biosensors. Finally, the results obtained using a sol-gel coated LPG of batch C are better than the previous ones even if they were achieved in a different condition (in serum) with a longer interaction time. This can be explained with the fact that the value of the overlay thickness related to LPGs of batch C is very close to the OOT (between B_2 and B_1 points in Figure S-5) thus exactly in the modal transition region of the considered LP_{07} mode.

Initial binding rate

The use of a sol-gel based film overlay has the advantage of increasing the sensitivity of LPGs and of decreasing the LOD. On the other hand, the combined use of serum as surrounding environment and of a sol-gel matrix, due to its intrinsic nanoporous nature, leads to an increase of the antibody-antigen binding interaction time. For the immunoassay performed in serum, the interaction time was increased from 20 minutes, used in the case of PBS, up to 1 hour and 10 minutes. This increase was necessary in order to allow the sensor to reach a stable value, as shown in Figure S-9 that details the IgG/anti-IgG binding interaction (normalized LPG λ_{res} evolution in time) at the antigen concentration of 1 mg L^{-1} for the immunoassay performed either in PBS (LPG of batch A, grey line) or in serum (LPG of batch C, black line). Both the curves show a typical exponential behavior with a steady state obtained in different times, 10 minutes in PBS and 40 minutes in serum. This lengthening can be ascribed to the higher complexity of the serum matrix with respect to simple PBS, which implies a decrease of the antigen mobility. Moreover, the increase of the response time from roughly 6–8 minutes and 14–16 minutes in PBS[18] and serum,[22] respectively, obtained with not coated LPGs, to roughly 10–12 minutes and

40–60 minutes in PBS and serum, respectively, obtained with coated LPGs, can depend on the electrostatic interactions between the film and charged or polar site of the analyte, and on both the granularity and homogeneity of the deposited film overlay.[31,34]

In order to reduce the time necessary for determining the concentration value of the target interacting with the sensing layer, the initial binding rate (IBR), which is the slope of the binding interaction during its first minutes, was considered.[14] For this purpose, the evaluation of the IBR was carried out from the initial response of the sensor by discarding the first three measuring points, corresponding to the initial and almost instantaneous shift of LPG λ_{res} due to the bulk RI change of the solution, and by considering the subsequent 15 ones during the first phase of the binding interaction for all the anti-IgG concentrations (overall measuring time of about 3 minutes). With these experimental points, a linear regression was performed and the IBR, expressed in nm min^{-1}, was evaluated. An example of this procedure is shown in Figure S-10, which accounts for the binding interaction between the IgG and anti-IgG (1 mg L^{-1}) in human serum using the coated LPG of batch C. In order to avoid any temperature-induced effect on the sensor response, all the solutions injected into the flow cell were stabilized in advance at the same temperature of the flow cell before their injection.

By reporting the IBR as a function of the antigen concentration for analysis two sol-gel coated LPGs, one of batch A (assay performed in PBS) and another of batch C (assay performed in serum), it was possible to draw the calibration curve of the biosensor as a function of this parameter (Figure 6). All the data of interest are gathered in Table S-1, along with the respective standard deviation.

Figure 6. Calibration curves of the proposed biosensor (IBR vs antigen concentration in logarithmic scale) obtained by using the same procedure but with different coated LPGs: LPG of batch A (red rhombuses) by performing the assay in PBS buffer, and of batch C (black triangles) by performing the assay in human serum. The dashed lines are the broken lines that connect the experimental points and are drawn with the purpose to provide a general view of the trends.

Although the two calibration curves of Figure 6 show data obtained from different titania-silica films and different matrices, the IBR increases in modulus similarly (within the error) with the concentration of the anti-IgG concentration. This demonstrates that the IBR is an alternative metric to determine the concentration of the analyte under investigation. Finally, it is worth pointing out that the negative sign of IBR is just related to the sensing mechanism governing the LPG that implies a decrease of the resonance wavelength when a biochemical interaction takes place (see eq. 1 and Figure 1).

CONCLUSIONS

The performances of sol-gel based titania-silica thin film overlay for LPGs have been assessed. They have been tested as effective and feasible optical platforms for label-free biosensing by means of the implementation of IgG/anti-IgG immunoassays. The analysis revealed that two analytical parameters, the wavelength shift at the end of the binding process and the initial binding rate during the first minutes of the binding process, can be used for the performance evaluation of the biosensors.

Thin film overlays were deposited by a simple and versatile DC technique. Since the performance of coated LPGs strongly depends on the overlay parameters (i.e. its refractive index and thickness), both the sol viscosity and the withdrawal speed were changed during the sensor

implementation in order to optimize the overlay thickness. Sensors with overlay thickness of 120–160 nm and RI of 1.7 RIU were manufactured and characterized. The best performance was achieved with an overlay thickness of 154 nm. In this case, a LOD of 8 μg L^{-1} (5.3 x 10^{-11} M) was attained with measurements in serum.

Sol-gel based titania-silica coated LPGs showed bulk refractive index sensitivity of the order of thousands of nm RIU^{-1} and a resolution of the order of 10^{-6} RIU in water environment. It is worth mentioning that these values are among the best of optical fiber LPG-based biosensors reported in literature up to now.[55,13] It is worth pointing out that this kind of sensor, which measures wavelength shifts as a function of RI changes, cannot directly be used for absolute RI measurements without a proper calibration, but it is perfectly suitable when examining time-series measurements for detecting small changes in RI, as here demonstrated.

Finally, the real effectiveness and feasibility of an LPG-based biosensor were proved by performing the immunoassay in human serum as a complex and real environment, which also confirmed the assay specificity.

ASSOCIATED CONTENT

Supporting Information.

An overview of the over-coupled LPGs. Data processing and analysis. Response of sol-gel based titania-silica coated LPGs to temperature variations. Thickness optimization of sol-gel based titania-silica coated LPGs. An example of the LPG spectrum before and after the annealing process. An example of the procedure for determining the LPG resonance wavelength. Schematic representation of the proposed assay protocol. An example of the LPG spectrum

before and after the film deposition. Simulated curves used for the optimization of the film overlay thickness as a function of both the surrounding RI and the overlay RI. An example of the LPG spectrum before and after the modal transition. Stability test of the sensor. An example of the antibody-antigen binding interaction obtained in buffer and in serum. An example of the used procedure to determine the IBR. This information is available free of charge via the Internet at http://pubs.acs.org/ .

AUTHOR INFORMATION

Corresponding Authors

* E-mail palas@cgcri.res.in (P. Biswas); Tel.: +91 332 483 8083. E-mail c.trono@ifac.cnr.it (C. Trono); Tel.: +39 055 522 6359.

Author Contributions

All the authors have given their contribution to the manuscript and approval to the final version of the manuscript.

Notes

The authors declare no competing financial interest.

ACKNOWLEDGMENT

This research study was supported by the Joint Research Proposal (No.22/EU/Italy/CNR/proj./2012) under CNR, Italy – CSIR, India Bilateral S&T Programme, entitled “Development of Long Period Grating (LPG) based immunoassay for bio-sensing applications”. F.C. wishes to thank the Italian Minister of University and Research (MIUR)

under the grant N. RBFR122KL1. S.T. wishes to thank the European Community for the project Hemospec (FP7 - 611682).

REFERENCES

(1) Hunt, H. K.; Armani, A. M. *Nanoscale* **2010**, *2*, 1544–1559.

(2) Fan, X.; White, I. M.; Shopova, S. I.; Zhu, H.; Suter, J. D.; Sun, Y. *Anal. Chim. Acta* **2008**, *620*, 8–26.

(3) Homola, J. *Chem. Rev.* **2008**, *108*, 462–493.

(4) Šípová, H.; Zhang, S.; Dudley, A. M.; Galas, D.; Wang, K.; Homola, J. *Anal. Chem.* **2010**, *82*, 10110–10115.

(5) Voisin, V.; Pilate, J.; Damman, P.; Mégret, P.; Caucheteur, C. *Biosens. Bioelectron.* **2014**, *51*, 249–254.

(6) Willets, K. A.; Van Duyne, R. P. *Annu. Rev. Phys. Chem.* **2007**, *58*, 267–297.

(7) Estevez, M. C.; Otte, M. A.; Sepulveda, B.; Lechuga, L. M. *Anal. Chim. Acta* **2014**, *806*, 55–73.

(8) Queirós, R. B.; Silvia, S. O.; Noronha, J. P.; Franzão, O.; Jorge, P.; Aguilar, G.; Marques, P. V. S.; Sales, M. G. F. *Biosens. Bioelectron.* **2011**, *26*, 3932–3937.

(9) Kindt, J. T.; Bailey, R. C. *Curr. Opin. Chem. Biol.* **2013**, *17*, 818–826.

(10) Dante, S.; Duval, D.; Farina, D.; González-Guerrero, A. B.; Lechuga, L. M. *Laser Photon. Rev.* **2015**, *9*, 248–255.

(11) Wang, X. D.; Wolfbeis, O. S. *Anal Chem.* **2013**, *85*, 487–508.

(12) Lepinay, S.; Staff, A.; Ianoul, A.; *Biosens. Bioelectron.* **2014**, *52*, 337–344.

(13) Baldini, F.; Brenci, M.; Chiavaioli, F.; Giannetti, A.; Trono, C. *Anal. Bioanal. Chem.* **2012**, *402*, 109–116.

(14) DeLisa, M. P.; Zhang, Z.; Shiloach, M.; Pilevar, S.; Davis, C. C.; Sirkis, J. S.; Bentley, W. E. *Anal. Chem.* **2000**, *72*, 2895–2900.

(15) Carrasquilla, C.; Xiao, Y.; Xu, C. Q.; Li, Y.; Brennan, J. D. *Anal. Chem.* **2011**, *83*, 7984–7991.

(16) Yang, R. Z.; Dong, W. F.; Meng, X.; Zhang, X. L.; Sun, Y. L.; Hao, Y. W.; Guo, J. C.; Zhang, W. Y.; Yu, Y. S.; Song, J. F.; Qi, Z. M.; Sun, H. B. *Langmuir* **2012**, *28*, 8814–8821.

(17) Pilla, P.; Sandomenico, A.; Malachovská, V.; Borriello, A.; Giordano, M.; Cutolo, A.; Ruvo, M.; Cusano, A. *Biosens. Bioelectron.* **2012**, *31*, 486–491.

(18) Chiavaioli, F.; Trono, C.; Giannetti, A.; Brenci, M.; Baldini, F. *J. Biophotonics* **2014**, *7*, 312–322.

(19) Korposh, S.; Chianella, I.; Guerreiro, A.; Caygill, S.; Piletsky, S.; James, S. W.; Tatam, R. P. *Analyst* **2014**, *139*, 2229–2236.

(20) Tripathi, S. M.; Bock, W. J.; Mikulic, P.; Chinnappan, R.; Ng, A.; Tolba, M.; Zourob, M. *Biosens. Bioelectron.* **2012**, *35*, 308–312.

(21) Wang, Z.; Heflin, J. R.; Van Cott, K.; Stolen, R. H.; Ramachandran, S.; Ghalmi, S. *Sens. Actuators B* **2009**, *139*, 618–623.

(22) Chiavaioli, F.; Biswas, P.; Trono, C.; Bandyopadhyay, S.; Giannetti, A.; Tombelli, S.; Basumallick, N.; Dasgupta, K.; Baldini, F. *Biosens. Bioelectron.* **2014**, *60*, 305–310.

(23) Erdogan, T. *J. Opt. Soc. Am. A* **1997**, *14*, 1760–1773.

(24) Patrick, H. J.; Kersey, A. D.; Bucholtz, F. *J. Lightwave Technol.* **1998**, *16*, 1606–1612.

(25) Del Villar, I.; Matías, I. R.; Arregui, F. J.; Lalanne, P. *Opt. Express* **2005**, *13*, 56–69.

(26) Rees, N. D.; James, S. W.; Tatam, R. P.; Ashwell, G. J. *Opt. Lett.* **2002**, *27*, 686–688.

(27) Keith, J.; Hess, L. C.; Spendel, W. U.; Cox, J. A.; Pacey, G. E. *Talanta* **2006**, *70*, 818–822.

(28) Ishaq, I. M.; Quintela, A.; James, S. W.; Ashwell, G. J.; Lopez-Higuera, J. M.; Tatam, R. *Sens. Actuators B Chem.* **2005**, *107*, 738–741.

(29) Wang, Z.; Heflin, J. R.; Stolen, R. H.; Ramachandran, S. *Opt. Express* **2005**, *13*, 2808–2813.

(30) Pilla, P.; Trono, C.; Baldini, F.; Chiavaioli, F.; Giordano, M.; Cusano, A. *Opt. Lett.* **2012**, *37*, 4152–4154.

(31) MacCraith, B. D. *Sens. Actuators B* **1993**, *11*, 29–34.

(32) Lee, J. E.; Saavedra, S. S. *Anal. Chim. Acta* **1994**, *285*, 265–269.

(33) Bullen, C.; Mulvaney, P.; Sada, C.; Ferrari, M.; Chiasera, A.; Martucci, A. *J. Mater. Chem.* **2004**, *14*, 1112–1116.

(34) MacCraith, B. D.; McDonagh, C. M.; O'Keeffe, G.; McEvoy, A. K.; Butler, T.; Sheridan, F. R. *Sens. Actuators B* **1995**, *29*, 51–57.

(35) Davies, E.; Viitala, R.; Salomäki, M.; Areva, S.; Zhang, L.; Bennion, I. *J. Opt. A: Pure Appl. Opt.* **2009**, *11*, 015501.

(36) Smietana, M.; Koba, M.; Mikulic, P.; Bock, W. J. *Meas. Sci. Technol.* **2014**, 25, 114001.

(37) Smietana, M.; Mysliwiec, M.; Mikulic, P.; Witkowski, B. S.; Bock, W. J. *Sensors* **2013**, 13, 16372–16383.

(38) Smietana, M.; Koba, M.; Brzozowska, E.; Krogulski, K.; Nakonieczny, J.; Wachnicki, L.; Mikulic, P.; Godlewski, M.; Bock, W. J. *Opt. Express* **2015**, 23, 8441–8453.

(39) Gu, Z.; Xu, Y.; Gao, K. *Opt. Lett.* **2006**, *31*, 2405–2407.

(40) Hill, K. O.; Meltz, G. *J. Lightwave Technol.* **1997**, *15*, 1263–1276.

(41) Erdogan, T.; Mizrahi, V.; Lemaire, P. J.; Monroe, D. *J. Appl. Phys.* **1994**, *76*, 73–80.

(42) Biswas, P.; Basumallick, N.; Dasgupta, K.; Bandyopadhyay, S. *J. Lightwave Technol.* **2014**, *32*, 2072–2078.

(43) Sarkar, S.; Roy, R. D.; Biswas, P. K.; Bhadra, S. K; Jana, S. *International Journal of Engineering and Innovative Technology* (IJEIT), **2014**, *3*, 212–218.

(44) Cusano, A.; Iadicicco, A.; Pilla, P.; Contessa, L.; Campopiano, S.; Cutolo, A.; Giordano, M. *Opt. Express* **2006**, *14*, 19–34.

(45) Trono, C.; Baldini, F.; Brenci, M.; Chiavaioli, F.; Mugnaini, M. *Meas. Sci. Technol.* **2011**, *22*, 075204.

(46) Zhou, W.; Mandia, D. J.; Barry, S. T.; Albert, J. *Opt. Lett.* **2015**, 40, 1713–1716.

(47) Chryssis, A. N.; Saini, S. S.; Lee, S. M.; Dagenais, M. *IEEE Photon. Technol. Lett.* **2006**, 18, 178–180.

(48) Brinker, C. J.; Scherer, G. W. *Sol-gel science*; Academic Press Inc.:San Diego (CA), 1990.

(49) Cheung, C. S.; Topliss, S. M.; James, S. W.; Tatam, R. P. *J. Opt. Soc. Am. B* **2008**, 25, 897–902.

(50) Faustini, M.; Louis, B.; Albouy, P. A.; Kuemmel, M.; Grosso, D. *J. Phys. Chem. C* **2010**, 114, 7637–7645.

(51) Sonawane, R. S.; Hegde, S. G.; Dongare, M. K. *Mater. Chem. Phys.* **2003**, 77, 744–750.

(52) Sil, D.; Deb Roy, R.; Jana, S.; Mukherjee, R.; Bhadra, S. K.; Biswas, P. K. *J. Sol-Gel Sci. Technol.* **2011**, 59, 117–127.

(53) James, S.W.; Tatam, R. P. *Meas. Sci. Technol.* **2003**, 14, R49–R61.

(54) Dudley, R. A.; Edwards, P.; Ekins, R.P.; Finney, D.J.; McKenzie, I.G.; Raab, G.M.; Rodbard, D.; Rodgers, R.P. *Clin. Chem.* **1985**, 31, 1264–1271.

(55) Gouveia, C. A. J.; Baptista, J. M.; Jorge, P. A. S. In *Current developments in optical fiber technology*; Harun, S. W., Arof, H., Eds.; InTech (online publisher), 2013; pp 345–373.

TABLE OF CONTENTS GRAPHIC